Biophysical Journal Volume 76 April 1999 2081–2089

Dynamical Properties of Phospholipid Bilayers from Computer Simulation

Ulrich Essmann* and Max L. Berkowitz#

*GMD–German National Research Center for Information Technology, D-53754 St. Augustin, Germany, and #Department of Chemistry, University of North Carolina, Chapel Hill, North Carolina 27599 USA

ABSTRACT We present the results of a 10-ns molecular dynamics simulation of a dipalmitoylphosphatidylcholine/water system. The main emphasis of the present study is on the investigation of the stability over a long time and the dynamic properties of the water/membrane system. The motion of the lipid molecules is characterized by the center of mass movement and the displacement of individual atom groups. Because of the slow movement of the headgroup atoms, their contributions to the dipole potential vary slowly and with a large amplitude. Nevertheless, the water molecules compensate the strong fluctuations and maintain an almost constant total dipole potential. From the lateral displacement of the center of masses, we calculate the lateral diffusion coefficient to be $D_{\mathrm{lat}} = (3 \pm 0.6) \times 10^{-7}$ cm^2/s, in agreement with neutron scattering results. The rotational motion is also investigated in our simulations. The calculated value for the rotational diffusion coefficient parallel to the molecular long axis, $D_{\parallel} = (1.6 \pm 0.1) \times 10^{8}$ s^{-1}, is in good agreement with the experiment.

INTRODUCTION

Over the last 15 years an increasing number of computer simulation studies have contributed to the understanding of the molecular structure of membranes (for reviews see Pastor, 1994; Mouritsen and Jorgensen, 1997; Tieleman et al., 1997; Tobias et al., 1997). Because the main focus of these studies is on structural properties, dynamical properties of the membranes have usually been neglected. This is unfortunate, because the fluid mosaic model of Singer and Nicholson strongly suggests that membrane fluidity plays a major role in the biological properties of the membrane (Singer and Nicholson, 1972; Jacobson et al., 1995). A notable exception is the work of Pastor and Feller (1996), in which the authors discuss the time scales of lipid dynamics and the relationship of these time scales to molecular dynamics. The range of time scales for different types of molecular motions in membranes is impressively large. On the shortest time scales are intermolecular vibrations, with a period on the order of 10^{-14} s, and on the other end of the scale are transbilayer flip-flop processes across the bilayer, with a typical time scale of minutes to hours (Blume, 1993). Clearly, with detailed atomistic simulation techniques, only the faster motions are currently accessible. Another limitation to the study of dynamical processes arises from the fact that many slower processes are collective excitations involving large spatial domains. Current molecular simulations, however, rarely exceed 100 Å in any direction.

In the present study we attempt to investigate the dynamical properties of individual lipid molecules. To cover a broad spectrum of modes we extended the total simulation time to 10 ns. As we shall see, this allows the calculation of experimentally observed transport properties such as lateral and rotational diffusion coefficients. The large time scale also allows us to investigate the stability of the membrane system. It has recently been questioned whether lipid-water systems are mechanically stable in constant volume simulations (Shinoda et al., 1997). The claim was that only constant pressure simulations can lead to stable trajectories. However, as we shall see below, a reasonable choice of box parameters leads to stable trajectories in a constant volume ensemble.

Another issue that can be investigated by performing long time simulations is the issue of the validity of certain results obtained previously from relatively short time simulations on membranes. Because of the great internal flexibility of the lipid molecules, individual groups, for example, the headgroup or the lipid chains, move with large amplitudes. This is of particular concern for the headgroups because the headgroups produce an electric dipole potential of several volts. Therefore the question arises whether the large movements of the headgroup lead naturally to large fluctuations of the dipole potential, thereby rendering the results of shorter simulations of several hundred picoseconds meaningless.

METHODOLOGY

Because the computational protocol of the present calculation is similar to that of our previous study (Essmann et al., 1995a) we repeat here only a few characteristics of this protocol. Sixty-four dipalmitoylphosphatidylcholine (DPPC) molecules and 1315 water molecules are arranged in the primary simulation cell to form a bilayer/water system. By applying three-dimensional periodic boundary conditions, a multilamellar system is generated. This choice seems to be reasonable because many experiments have been performed on multilayer systems. The choice of the number of water molecules corresponds to 20.5 water molecules/lipid or 33.5% water fraction. Recent x-ray experiments on the

---

Received for publication 27 April 1998 and in final form 5 January 1999.

Address reprint requests to Dr. Ulrich Essmann, GMD–SCAI, German National Research Center for Information Technology, Schloss Birlinghoven, D-53754 St. Augustin, Germany. Tel.: 49-2241-14-2795; Fax: 49-2241-14-2656; E-mail: essmann@gmd.de.

0006-3495/99/04/2081/09 $2.00

structure of DPPC bilayers found that important physical characteristics such as bilayer thickness and area per headgroup remain conserved between a water content of 15.5 waters/lipid and the hydration limit of 28 waters/lipid (Nagle et al., 1996).

Therefore, the physical characteristics of our system should be very similar to those of a fully hydrated sample. The area per headgroup is set at 65.8 Å^2. This value is somewhat larger than the recent experimental value (Nagle et al., 1996) of 62.9 ± 1.3 Å^2; however, given that the simulation temperature is 60°C whereas the experiments are performed at 50°C, this value is within the range of experimental uncertainties. The bilayer repeat distance was set at 56.8 Å, in agreement with experimental data for this level of hydration (Ruocco and Shipley, 1982). The present simulation is an extension of the large liquid crystalline simulation of our previous paper. The trajectories are calculated using a time step of 2 fs. The total length of this run is 10 ns.

The lipid molecules are represented using the united atom model with the STUB parameter set of the PARM91 file of AMBER (Pearlman et al., 1995), except for the dihedral angles of the alkane chains, which are described by the Ryckaert-Bellemans potential (Ryckaert and Bellemans, 1975). All intramolecular bond lengths are fixed with the SHAKE algorithm (Ryckaert et al., 1977). Fractional charges for the lipid molecules were calculated with GAUSSIAN92 (Frisch et al., 1992) with a 6–31G* basis set; the values are given in our previous work (Essmann et al., 1995a). For the calculation of the Coulomb interactions, the recently invented particle mesh Ewald (PME) method of Darden et al. (Darden et al., 1993; Essmann et al., 1995b) was used.

STABILITY OF THE SYSTEM

In many membrane simulations the time covered is on the order of a few hundred picoseconds. Because the assembly and disassembly of these complex systems require much longer time scales, it might very well be that the systems under study form a bilayer structure only as a consequence of the initial setup of the simulated system.

We use here the atom distribution along the bilayer normal as an indication of a disintegration of the bilayer. To analyze the time evolution of the system and to assess the size of the fluctuations in these quantities, we divide the whole run into 33 pieces of 300 ps each. We calculate the atom distribution for the following four characteristic groups: 1) the nitrogen atoms, 2) the phosphorous atoms, 3) the carbonyl groups and 4) the water molecules. To calculate the atom distributions we divide the system into *N* slices perpendicular to the *z* axis. For each slice we calculate the atomic density for every one of the 33 time intervals mentioned above. Therefore, for each of the *N* slices we calculate the average and the standard deviation of the 33 values. The resulting distribution functions plus the standard deviations for these four distribution functions are displayed in Fig. 1. To make the comparison between the two monolayers easier, we plot the center of the water slab in the middle of the plot at ~28.4 Å. The tails of the lipid molecules are on the left and right sides of the plots.

As one can see from Fig. 1, the fluctuations in the N-, P-, and CO- distribution functions reach a level of 25–35%. Furthermore, as can be seen from these plots, the distribution functions are not symmetrical. To quantify this asymmetry we fitted Gaussians to the distribution functions. We find an almost identical asymmetry For the widths of the P- and CO- distributions (σ = 3.27 Å and σ = 3.70 Å for phosphorous and σ = 3.31 Å and σ = 3.75 Å for the carbonyl groups), which both amount to 13%. For nitrogen the Gaussians are much broader (σ = 4.91 Å and σ = 5.33 Å), and the asymmetry is only 9%. This observation is significant, as it indicates that during a simulation an asymmetry, which might be induced during the setup procedure, for example, can persist for a very long time.

To be able to find long time trends in these functions, we compared the atomic densities of the first 300 ps with those of the last 300 ps and the average densities (not shown). A broadening of the atom distributions during the whole run would indicate an instability. A sharpening, on the other hand, would indicate that the interface is better defined than was described in our previous study and that the membrane

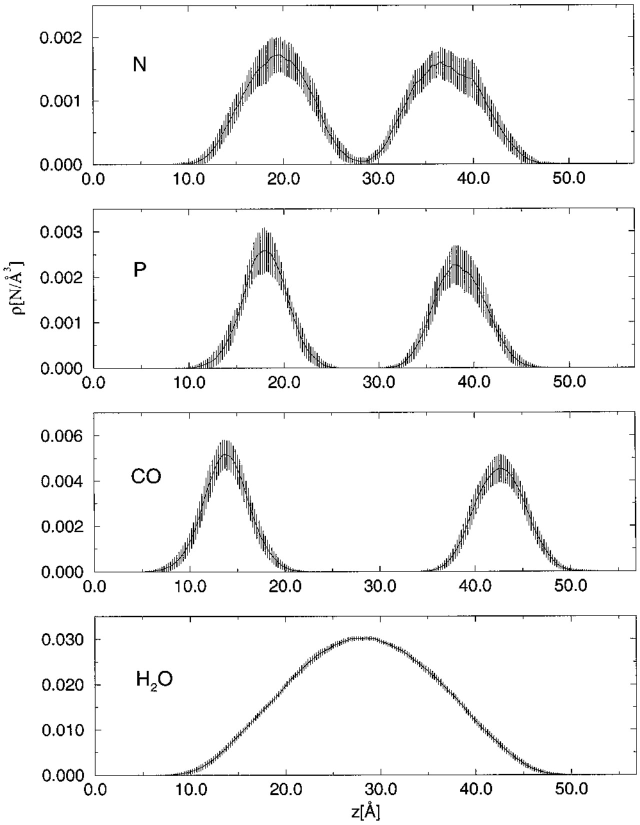

FIGURE 1 Atom distributions for four selected groups. The vertical lines indicate the variance calculated from the division of the whole run into 33 pieces with lengths of 300 ps each, as described in the text.

interface is not as rough. We found a slight broadening of the phosphorous distribution, which was in contrast, however, to a slight sharpening of the carbonyl distribution functions. Comparing the distribution functions of the first 300 ps and the last 300 ps with the average values and their fluctuations, we conclude that the observed trends are merely an expression of random fluctuations rather than long time trends.

Recently the concern has been raised that membrane systems cannot be simulated with a fixed box geometry (Shinoda et al., 1997). The present result, however, indicates that for a reasonable choice of physical parameters, the stability of the system is preserved. The disadvantage of a simulation with a fixed box geometry is the need to specify the three box lengths. In general the three box angles have to be specified too; however, except for crystal simulations, they are usually set at 90°. Assuming that the system is isotropic within the plane of the membrane, one can set the two box lengths in the lateral dimension equal to each other. Furthermore, setting the box angles at 90°, there are still two parameters left, the area per headgroup and the bilayer repeat distance. In the case of pure DPPC membranes in water these two parameters can be obtained, with reasonable accuracy, from experimental data. However, in many interesting cases, such as the incorporation of peptides or proteins into membranes, the total membrane area is not known and constant pressure simulations are necessary (Feller et al., 1995).

FLUCTUATIONS IN THE ELECTROSTATIC MEMBRANE POTENTIAL

The membrane dipole potential is thought to play an important role in regulating not only the structure and function of membranes (Brockman, 1994), but even more complex processes such as the adsorption of proteins (Nordera et al., 1997). Experimentally this quantity is rather difficult to measure (Brockman, 1994). In general for DPPC bilayers, a value between −0.2 V (Gawrisch et al., 1992) and −0.4 V (Pickar and Benz, 1978) is obtained from the measurements. Membrane dipole potentials have also been calculated in molecular dynamics simulations. In our previous study the dipolar potential was calculated from a 300-ps simulation. Because of the zwitterionic nature of the headgroup, a dipole potential is associated with these headgroups. This dipole potential, in turn, leads to an ordering of adjacent water molecules. Because the conformations of the lipid headgroups vary strongly, one might expect that the dipole potential varies strongly over time as well. This could also explain the differences between reported values (Marrink et al., 1993; Essmann et al., 1995a).

To study the character of the fluctuations in the dipole potential we divided the total run into blocks of 300 ps length and calculated the contribution of the headgroups, the contribution of the water molecules to the dipole potential, and the total potential according to the formula

$$\psi(z) - \psi(0) = -\frac{1}{\epsilon_0}\int_0^z \mathrm{d}z' \int_0^{z'} \rho(z'')\mathrm{d}z'' \qquad (1)$$

where $\psi(z)$ denotes the dipole potential and $\rho(z)$ the charge density. The z axis is chosen to be parallel to the membrane normal.

In Fig. 2 the contributions from the lipid headgroups as well as from the water molecules are shown together with the total potential. The electrostatic potential of the headgroup fluctuates by ±0.24 V around an average value of 2.24 V, and similarly, the fluctuations of the electrostatic potential of the water are ±0.23 V around the average value of −3.20 V, whereas the fluctuations of the total electrostatic potential around the average value of −0.96 V are only ±0.03 V and therefore are one order of magnitude smaller.

This result can be rationalized as followings. Because of the slowness of the motion of the headgroups, the electrostatic potential of the headgroups fluctuates on the time scale of several nanoseconds. In response to these fluctuations, the water molecules reorient themselves and compensate for the fluctuating field. However, this reorientation of the water molecules happens on a much faster time scale, so that the potential is balanced overall. It should be emphasized that the fact that the total potential stays constant over time is not a result of the use of the Ewald summation, because the individual components fluctuate very strongly.

DIFFUSION OF LIPID MOLECULES

Using the data obtained from the neutron scattering experiment, it was proposed that the in-plane motion of the whole lipids consists of two parts: local diffusion of a lipid molecule in its cage and long-range diffusional jumps between adjacent sites (Sackmann, 1995). The corresponding diffu-

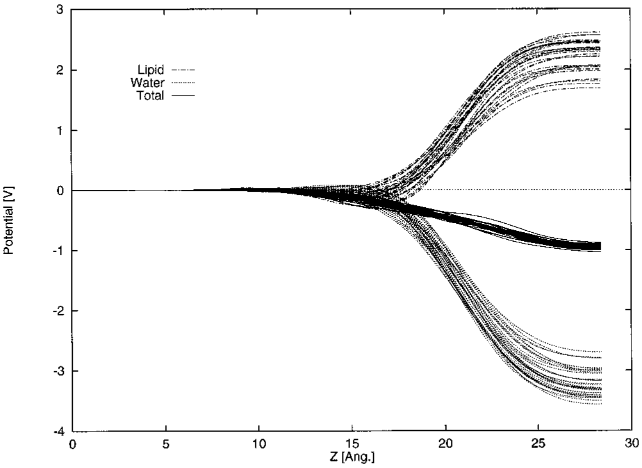

FIGURE 2 The total membrane potential and the components due to the water and the headgroup contributions.

sion coefficients for DPPC at 12 wt% water and 60°C were measured to have values of $D_{\text{loc}} = 2 \times 10^{-7}$ cm^2/s and $D_{\text{lat}} = 1 \times 10^{-7}$ cm^2/s. The diffusion coefficients can be also obtained from molecular dynamics simulations as the ratio of the mean square displacement (MSD) $(\vec{r}(t) - \vec{r}(0))^2$ to time in the limit of large times:

$$D = \lim_{\tau \to \infty} \frac{\langle |\vec{r}(t_o + \tau) - \vec{r}(t_o)|^2 \rangle}{2 N_f \tau} \tag{2}$$

The brackets indicate an average over different times t_o and all particles. The parameter N_f describes the number of translational degrees of freedom. For an isotropic liquid it is three, whereas for the case of the lateral diffusion of a lipid within a quasi-two-dimensional bilayer, it is two.

For the practical calculation it is also important to specify the particular reference point within the molecule for which the MSD is calculated. Even though in the limit of infinite time differences τ the choice of the reference point is irrelevant, for finite times the reported MSD might be different because of the slowness of intramolecular motions. We will report first the MSD for the center of mass (COM) and will return to the motion of individual atoms later.

To see if we have a local diffusional motion on a shorter time scale and a jump-type motion on a longer time scale, we divided the whole run of 10 ns into four pieces of 2.5 ns each. For every piece of 2.5 ns we calculated the MSD up to $\tau = 500$ ps. The plots of these MSDs are shown in Fig. 3. By fitting straight lines to the four curves in the region 300–500 ps, we obtained the following values for the diffusion coefficients: $D = 2.26$, 3.70, 2.76, and 2.51×10^{-7} cm^2/s, with an average value of $D = 2.83 \times 10^{-7}$ cm^2/s and an error of 0.63×10^{-7} cm^2/s. If we calculate the MSD using the data from the whole 10 ns of the simulation with a maximum $\tau = 3$ ns and fit the curve to a straight line on the interval 1.5–3.0 ns (see Fig. 4), we get the value $D = 3.14 \times 10^{-7}$ cm^2/s. If we assume that the error is on the same order of magnitude as in the analysis given above, we arrive at a value of $D = (3 \pm 0.6) \times 10^{-7}$ cm^2/s. As we can see, the two values obtained from an analysis with a shorter τ and with a longer τ are close to each other. The closeness of the two values for the short-time diffusional motion and longer-time motion suggests that there are no two regimes in the lateral diffusion. To check this we observed the trajectories of the COMs of the lipid molecules, some of which are shown in Fig. 5 in a "stroboscopic picture." In this picture we place a dot marking the x and y coordinates of the COM of the phospholipid molecules every 40 ps. Connecting these dots gives us a representation for the projection of the COM trajectory into the x,y plane over a certain amount of time. As we can see from the figure, the trajectories show that lipids undergo ordinary diffusional motion on the time scale considered in this simulation. The depicted trajectories are typical for molecules in a liquid state and do not indicate local cage motion and jumps between cages.

The values for the diffusion coefficients we obtained from our simulations are in reasonable agreement with the values obtained from the neutron scattering experiments given above (Pfeiffer et al., 1989; König et al., 1992; Sackmann, 1995). We compare our results with results from neutron scattering experiments, because the time scale as well as the length scales match those of molecular simulations. Most other techniques cover either much larger time scales and/or much larger length scales. The larger time or length scales could possibly cover phenomena not included in our simulation.

To get a better feel for the dynamics on different time scales, we looked at "stroboscopic pictures" of the trajectories of the COM of the phospholipid molecule every 4 ps for a time interval of 100 ps and a time interval of 1 ns and every 40 ps for a time interval of 10 ns. This is done in Fig.

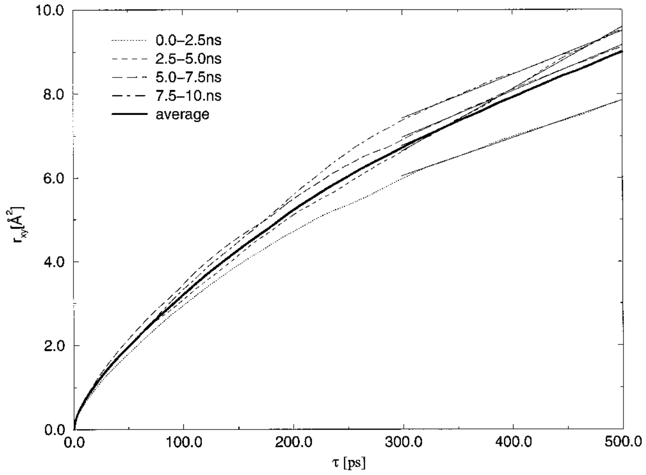

FIGURE 3 The mean squared displacement (MSD) for the COM in the x,y plane. The whole simulation was broken into four pieces of 2.5 ns each. The MSD for each of the four pieces as well as the average MSD are shown. For the interval between 300 ps and 500 ps, the straight lines represent a linear least-squares fit to these curves.

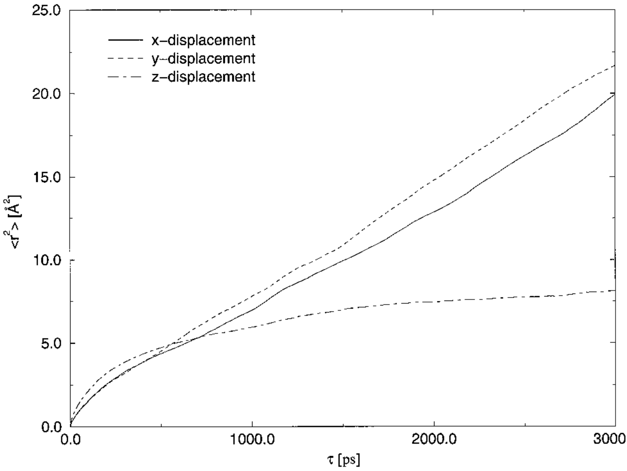

FIGURE 4 The MSD for the whole run calculated for the three coordinates separately.

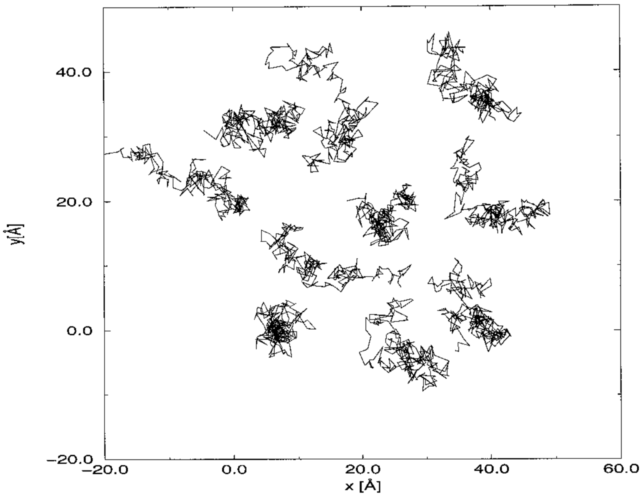

FIGURE 5 "Stroboscopic picture" of the COM of 10 selected lipids within the *x*,*y* plane. These lipids were selected so that their paths are well separated. The paths were traced during the entire simulation. To avoid the interruption of trajectories, periodic boundary conditions were not applied.

6, where trajectories are shown for the time interval of 100 ps, 1 ns, and 10 ns.

As we can see from the top panel of Fig. 6, over 100 ps, the COM are not displaced very far from the initial positions, such that the motion of the COM in the lateral direction over this time period is reminiscent of a glassy state. Even during the 1-ns time period we do not observe a large displacement of COMs from their initial positions (Fig. 6, *middle panel*). The picture changes quite substantially in the bottom panel of Fig. 6, where the trajectories of the COMs clearly show that the membrane layer is liquid. This view is supported by Fig. 5, which shows that some lipids moved quite substantially during the course of the simulation, whereas others remained close to their initial position, which is the behavior expected for Brownian motion. On average we observed that the particles moved ~12 Å over the course of the simulation, a distance larger than the next-neighbor distance.

In addition to the study of lateral motion, we also studied the motion of membrane molecules in the perpendicular z direction. Thus in Fig. 4 we plot the MSDs for the x, y, and z directions. As we can see, the MSDs for the x and y directions are approximately equal. The MSD in the z direction, however, is bound with a maximum value of $\Delta z^2 \approx 7.4$ Å^2. This value agrees with the neutron scattering value of $\Delta z \approx 2.5$ Å (Sackmann, 1995).

Furthermore, we calculated the MSD for the nitrogen atoms of the headgroups and the terminal methyl groups of the Sn1 and Sn2 chains. The MSD in the z direction of these groups as well as the corresponding quantity for the COM are shown in Fig. 7. There is a striking difference between the z displacement of the COM and the individual groups. The COM displacement reaches a plateau value after ~1 ns. However, the displacement of the individual groups reaches a maximum value only after 4–6 ns. Furthermore, the amplitude of this motion is rather different. Whereas for the COM we find a maximum MSD in the z direction of ~8 Å^2, the maximum values for the two terminal methyl groups are on the order of 30–35 Å^2. Similarly, the MSD in the z direction for the nitrogen atoms is ~25 Å^2. These MSDs correspond to absolute displacements of 5–6 Å.

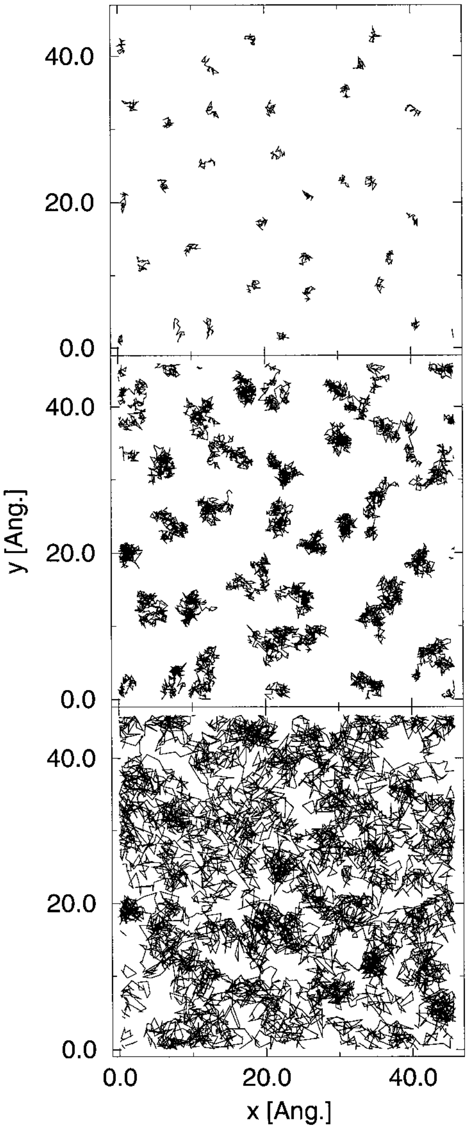

FIGURE 6 "Stroboscopic picture" of the trajectories of one monolayer. (*Top*) Over a time period of 100 ps. Time interval between two dots: 4 ps. (*Middle*) Over a time period of 1 ns. Time interval between two dots: 4 ps. (*Bottom*) Over a time period of 10 ns. Time interval between two dots: 40 ps.

The displacements in the z directions are predicted by the so-called protrusion model of Israelachvili and Wennerström (1990). This model is an attempt to explain the strong repulsive interaction between membranes over short distances. Experimentally it has been observed (LeNeveu et al., 1976; Rand and Parsegian, 1989) that at small separations, a repulsive interaction between opposing bilayer surfaces varies exponentially with distance. In the model of Is-

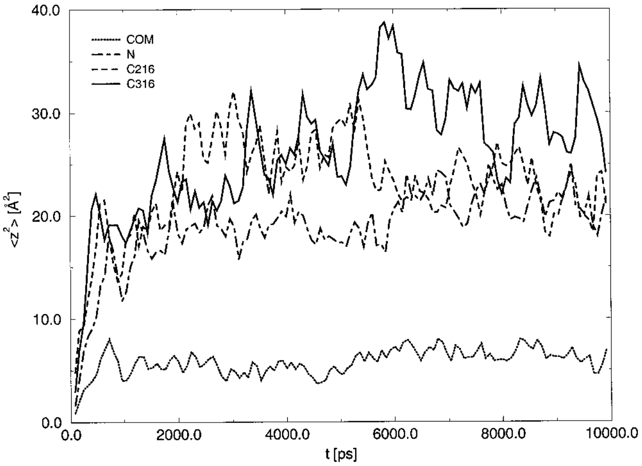

FIGURE 7 The mean squared displacement parallel to the bilayer normal for individual groups of the lipid molecules with respect to the initial configuration. The quantities displayed are averaged over the number of molecules. For these graphs periodic boundary conditions were applied.

raelachvili and Wennerström (1990) the movements of individual lipid molecules out of the membrane planes, so-called protrusions, are responsible for this force. If two membranes approach each other, the movement of individual lipid molecules out of the membrane plane is restricted by the presence of the lipid molecules of the approaching membrane. The presence of the opposing membrane therefore limits the configurational space of the lipid molecules. Assuming that the free energy of a protrusion increases linearly with its height and then using a Boltzmann ansatz for the height distribution lead to an exponentially varying repulsive force.

The above-mentioned numbers for the movements out of the membrane plane look rather short at first. However, as has been shown in a previous publication (Essmann et al., 1995a), even at a hydration level of 20.5 water molecules/lipid, individual headgroups come rather close. At this hydration level the width of the water slab according to the definition of McIntosh and Simon (1986) is ~12 Å, and a detailed analysis of the shortest distance between lipid molecules of opposing bilayers yields a similar length. At this distance the movement of the headgroup is sufficient to bring the nitrogen atoms in close proximity. Therefore the headgroups of the apposing bilayers start to restrict each other's available conformational space. At this point it is not possible to decide whether this effect is the cause of the hydration force, because the free energies involved in the hydration force are very small compared to the free energies measurable in molecular simulations.

OVERALL ROTATIONAL DYNAMICS

Another very important characteristic of the dynamics of lipid molecules in membranes is the rotational motion. This has been measured by NMR (Blume, 1993), electron spin resonance (Lange et al., 1985), and dielectric spectroscopy (Klösgen et al., 1996). Because of the nature of the lipid bilayer, the overall motion can be characterized by a rotation around an axis parallel to the bilayer normal and a so-called wobbling motion in which the long axis changes its orientation.

Because of the great internal flexibility of the lipids, it is not possible to define unambiguously the body fixed axes along which we can calculate the rotation of lipid molecules. To define the axes we first calculated the moments of inertia and the principal axes for each lipid molecule (Goldstein, 1980). The principal axis that makes the smallest angle with the bilayer normal is called the *z* axis. If the lipid molecules have two parallel Sn1 and Sn2 chains as often sketched in textbooks, then this would also be the axis associated with the smallest moment of inertia. However, in practice we observed that sometimes one of the other axes was associated with a smaller moment of inertia. We attribute this to conformations in which the two alkane chains were "spread apart." Because of the great internal flexibility we did not use the principal moments to define the *y* axis, but rather defined them as the normalized perpendicular component of the vector from the center of the Sn1 to the center of the Sn2 chain. The *x* axis is the unit vector forming a right-handed axis system.

To determine rotational diffusion constants we calculate the time correlation functions (Berne, 1971; Zannoni, 1994):

$$C^{\mathrm{LL}'}_{\mathrm{mn;m'n'}}(t) = \langle D^{\mathrm{L}}_{\mathrm{mn}}(0) D^{\mathrm{L}'*}_{\mathrm{m'n'}}(\mathrm{t}) \rangle \delta_{\mathrm{mm'}} \qquad (3)$$

where $D^{\mathrm{L}}_{\mathrm{mn}}$ is the Wigner rotation matrix. The formulas for calculating the $\langle D^{\mathrm{L}}_{\mathrm{mn}}(\delta\Omega) \rangle$ from the direction cosines of the body fixed axis system are given by Lynden-Bell and Stone (1989). In typical experiments only properties with $L = 1$ and $L = 2$ are studied. Therefore we limit our discussion to these quantities and to those in which $m = n$.

In Fig. 8 it can be seen that a fast initial decay of the correlation functions is followed by slower exponential decays. For the time interval between 700 and 3000 ps, straight lines can be fitted reasonably well to the logarithm of the correlation functions. To calculate diffusion coefficients from these data, we have to assume a model that connects these quantities with the observed correlation times. For a free Brownian rotor with cylindrical symmetry, one can derive a relationship between the correlation functions and the diffusion coefficients $D_\perp$ and $D_\|$ (Berne, 1971; Szabo, 1984):

$$C^{\mathrm{LL}'}_{\mathrm{mn;mn}}(t) = \frac{1}{(2L+1)} \exp[(-L(L+1)D_\perp - m^2(D_\| - D_\perp))t] \qquad (4)$$

The diffusion coefficient $D_\perp$ describes the wobbling motion of the molecular symmetry axis and $D_\|$ the spinning motion around the molecular long axis (*z* axis). With this equation we get for $L = 1, 2$ five equations for the two unknown diffusion coefficients (*m* and *n* assume only val-

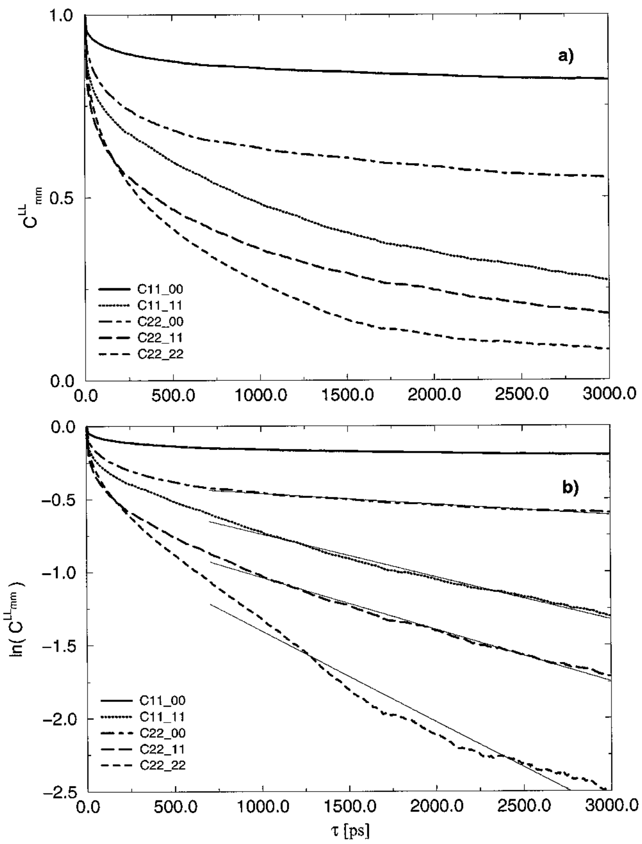

FIGURE 8 (*a*) The rotational autocorrelation functions of the lipid molecules. (*b*) Logarithm of the rotational autocorrelation function as a function of time. Included is a linear fit to the logarithm of these functions. Because of the fast initial decay only data points between 700 ps and 3000 ns are included in the fit.

ues between $-L$ and $+L$). One way to obtain the two diffusion coefficients would be to make a simultaneous least-squares fit of the diffusion coefficients to all five slopes. This approach yields a $D_\perp$ that is about one order of magnitude smaller than $D_\|$, in agreement with experimental results (Blume, 1993). To get a more reliable estimate of $D_\perp$, we first fit $D_\perp$ to the slopes of the two correlation functions with $m = 0$ and use this estimate to fit $D_\|$ to the three remaining slopes. To estimate the error we also calculate the variance. We use the values of $D_\perp$ and $D_\|$ to calculate the slopes of the correlation functions according to Eq. 4. Then we calculate the square of the difference to the observed slopes. This indicates how well the calculated $D_\perp$ and $D_\|$ fit the experimental data according to the free rotor model. Following this approach, we get the following values: $D_\perp = (1.2 \pm 0.2) \times 10^7\ \mathrm{s}^{-1}$, corresponding to a relaxation time of $\tau_\perp = (8 \pm 1) \times 10^{-8}$ s, and $D_\| = (1.6 \pm 0.1) \times 10^8\ \mathrm{s}^{-1}$, corresponding to a relaxation time of $\tau_\| = (6 \pm 0.4) \times 10^{-9}$ s.

These values agree well with measurements for DMPC membranes, which give (Mayer et al., 1990; Blume, 1993) a value of $\tau_\| = 5 \times 10^{-9}$ s at $T = 35°\mathrm{C}$. (Note that the gel-to-liquid crystalline phase transition for DMPC is 18°C lower than for DPPC (Cevc, 1993).) Furthermore, it is not possible to determine experimentally the precise value of $\tau_\perp$; however, it is believed to be in the nanosecond regime (Blume, 1993).

From a theoretical perspective the analysis in terms of the free rotor model is unsatisfactory, because it assumes a freely rotating cylinder. In a membrane this is certainly not the case. However, because the "wobbling motion" happens on a time scale much larger than that of the rotation around the long axis, it is nevertheless possible to calculate $D_\|$ reliably from the correlation functions given above and to provide at least an estimate of the magnitude of $D_\perp$.

Saffman and Delbrück (1975) estimated the ratio between the translational and rotational diffusion coefficient in membranes from the hydrodynamic theory. Within this model the membrane is treated as an infinite sheet of a viscous fluid (lipid) separating infinite regions of less viscous fluid (water). Within this sheet the diffusing particle is treaded as a cylinder. For the rotational diffusion coefficient $D_\|$ this model leads to the expression

$$D_\| = \frac{k_B T}{4\pi\mu a^2 h} \tag{5}$$

where a stands for the radius and h for the height of the cylinder and μ is the viscosity of the bilayer.

For the translational diffusion constant D_T Saffman and Delbrük obtained the following expression:

$$D_T = \frac{k_B T}{4\pi\mu h}\left(\log\left(\frac{\mu h}{\mu' a}\right) - \gamma\right) \tag{6}$$

where μ' is the viscosity of the surrounding fluid. Using $h = 20$ Å, $\mu = 1$ poise, $\mu' = 10^{-2}$ poise, and estimating the radius from the area per headgroup A as $a = (A/\pi)^{1/2} = 4.6$ Å and a value of 0.5772 for Euler's constant γ, one obtains the following for the ratio between the translational and rotational diffusion coefficient:

$$D_T/D_\| = \left(\log\left(\frac{\mu h}{\mu' a}\right) - \gamma\right) \cdot a^2 \tag{7}$$

$$= 1.1 \times 10^{-14}\ cm^2 \tag{8}$$

Using the numbers computed from our simulation, we obtain for this ratio a value of $D_T/D_\| \approx 2 \times 10^{-15}\ \mathrm{cm}^2$. Two comments have to be made here. First, the estimate of the radius of the lipid from the area per headgroup yields a very small value. Visual inspection of lipid configurations reveals that in most cases the two alkane chains are strongly disordered, and therefore the effective radius should be larger. Because there is no unambiguous way of calculating this effective radius, we considered only the simplest approximation. Second, a simplified hydrodynamic model of a complex phenomenon like the diffusion of a lipid molecule within a membrane can only be used with great caution. Keeping all of these limitations in mind, one can obtain a reasonable estimate with the simple continuum model.

SUMMARY

The long-time run of the present study demonstrates that the constant volume ensemble leads to stable simulations of membrane-water systems. As long as the geometry of the simulated system is chosen properly, the strong tendency of the water molecules to form hydrogen bonds is sufficient to maintain a stable water-membrane interface. The limitation of this approach is that only those systems can be studied for which enough experimental data are available to determine the geometry of the simulation cell.

Even though the internal flexibility leads to intramolecular fluctuations on a time scale of nanoseconds, certain quantities such as the dipole potential are rather stable and can be computed with good accuracies from much shorter simulations.

From our run it is also possible to calculate the diffusion coefficient of the lipid molecules. From the MSD we find a value of $D_{\mathrm{lat}} \approx (3 \pm 0.6) \times 10^{-7}$ cm^2/s for the lateral diffusion coefficient. This value agrees within a factor of 2 with the results obtained from quasielastic neutron scattering (Pfeiffer et al., 1989).

By calculating the MSD of the molecules perpendicular to the membrane surface, we find that lipid molecules as a whole protrude, on average, $\Delta z = 2.7$ Å out of the membrane plane. However, the nitrogen atoms of the headgroup move, on average, up to $\Delta z \approx 5$ Å into the water phase.

Finally we characterized the rotational motion of the lipid molecules by the rotational diffusion coefficient parallel and perpendicular to the molecule's long axis. The resulting parallel rotational diffusion coefficient agrees well with the experimentally determined values. The current characterization should therefore be supplemented by data from the NMR spectra to validate existing models and their interpretation.

We thank Prof. A. Geiger for helpful discussions, Dr. T. Darden of National Institute of Environmental Health Science for providing the PME code, and Dr. M. Crowley for the T3D/T3E version of the PME code. Furthermore, we thank Dr. K. Schweighofer for carefully reading the manuscript. The simulations were performed at the North Carolina Supercomputer Center and the HLRZ Supercomputing Center, Germany. Parts of this work have been conducted within the GMD research group Computational Methods in Chemistry of the High-Performance Computing Center (HLRZ).

This work was supported in part by the National Science Foundation and the National Institutes of Health.

REFERENCES

Berne, B. J. 1971. Time-dependent properties of condensed media. *In* Physical Chemistry, An Advanced Treatise, Vol. VIIIb. H. Eyring, D. Henderson, and W. Jost, editors. Academic Press, New York. 539–716.

Blume, A. 1993. Dynamic properties. *In* Phospholipids Handbook. G. Cevc, editor. Marcel Dekker, New York. 455–509.

Brockman, H. 1994. Dipole potential of lipid membranes. *Chem. Phys. Lipids.* 73:57–79.

Cevc, G. 1993. Appendix B: thermodynamic parameters of phospholipids. *In* Phospholipids Handbook. G. Cevc, editor. Marcel Dekker, New York. 939–956.

Darden, T., D. York, and L. Pedersen. 1993. Particle mesh Ewald: an *N*·log(*N*) method for Ewald sums. *J. Chem. Phys.* 98:10089–10092.

Essmann, U., L. Perera, and M. L. Berkowitz. 1995a. The origin of the hydration interaction of lipid bilayers from MD simulation of dipalmitoylphosphatidylcholine membranes in gel and liquid crystalline phases. *Langmuir.* 11:4519–4531.

Essmann, U., L. Perera, M. L. Berkowitz, T. Darden, H. Lee, and L. Pedersen. 1995b. A smooth particle mesh Ewald method. *J. Chem. Phys.* 103:8577–8593.

Feller, S. E., Y. Zhang, and R. W. Pastor. 1995. Computer simulation of liquid/liquid interfaces. II. Surface tension-area dependence of a bilayer and monolayer. *J. Chem. Phys.* 103:10267–10276.

Frisch, M. J., G. W. Trucks, M. Head-Gordon, P. M. W. Gill, M. W. Wong, J. B. Foresman, B. G. Johnson, H. B. Schlegel, M. A. Robb, E. S. Replogle, R. Gomperts, J. L. Andres, K. Raghavachari, J. S. Binkley, C. Gonzalez, R. L. Martin, D. J. Fox, D. J. Defrees, J. Baker, J. J. P. Stewart, and J. A. Pople. 1992. Gaussian 92, Revision E.2. Gaussian, Pittsburgh, PA.

Gawrisch, K., D. Ruston, J. Zimmerberg, V. A. Parsegian, R. P. Rand, and N. Fuller. 1992. Membrane dipole potentials, hydration forces, and the ordering of water at membrane surfaces. *Biophys. J.* 61:1213–1223.

Goldstein, H. 1980. Classical Mechanics, 2nd Ed. Addison-Wesley, Reading, MA.

Israelachvili, J. N., and H. Wennerström. 1990. Hydration or steric forces between amphiphilic surfaces? *Langmuir.* 6:873–876.

Jacobson, K., E. D. Sheets, and R. Simson. 1995. Revisiting the fluid mosaic model of membranes. *Science.* 268:1441–1442.

Klösgen, B., C. Reichle, S. Kohlsmann, and K. D. Kramer. 1996. Dielectric spectroscopy as a sensor of membrane headgroup mobility and hydration. *Biophys. J.* 71:3251–3260.

König, S., W. Pfeiffer, T. Bayerl, D. Richter, and E. Sackmann. 1992. Molecular dynamics of lipid bilayers studied by incoherent quasi-elastic neutron scattering. *J. Phys. II.* 2:1589–1615.

Lange, A., D. Marsh, K.-H. Wassmer, P. Meier, and G. Kothe. 1985. Electron spin resonance study of phospholipid membranes employing a comprehensive line-shape model. *Biochemistry.* 24:4383–4392.

LeNeveu, D. M., R. P. Rand, and V. A. Parsegian. 1976. Measurement of forces between lecithin bilayers. *Nature.* 259:601–603.

Lynden-Bell, R. M., and A. J. Stone. 1989. Reorientational correlation functions, quaternions and Wigner rotation matrices. *Mol. Simulation.* 3:271–281.

Marrink, S.-J., M. L. Berkowitz, and H. J. C. Berendsen. 1993. Molecular dynamics simulation of a membrane/water interface: the ordering of water and its relation to the hydration force. *Langmuir.* 9:3122–3131.

Mayer, C., G. Gröbner, K. Müller, K. Weisz, and G. Kothe. 1990. Orientation-dependent deuteron spin-lattice relaxation times in bilayer membranes: characterization of the overall lipid motion. *Chem. Phys. Lett.* 165:155–161.

McIntosh, T. J., and S. A. Simon. 1986. Hydration force and bilayer deformation: a reevaluation. *Biochemistry.* 25:4058–4066.

Mouritsen, O. G., and K. Jorgensen. 1997. Small-scale lipid-membrane structure: simulation versus experiment. *Curr. Opin. Struct. Biol.* 7:518–527.

Nagle, J. F., R. Zhang, S. Tristram-Nagle, W. Sun, H. Petrache, and R. M. Suter. 1996. X-ray structure determination of fully hydrated L_α phase DPPC bilayers. *Biophys. J.* 70:1419–1431.

Nordera, P., M. Dalla Serra, and G. Menestrina. 1997. The adsorption of *Pseudomonas aeruginosa* exotoxin A to phospholipid monolayers is controlled by pH and surface potential. *Biophys. J.* 73:1468–1478.

Pastor, R. W. 1994. Molecular dynamics and Monte Carlo simulations of lipid bilayers. *Curr. Opin. Struct. Biol.* 4:486–492.

Pastor, R. W., and S. E. Feller. 1996. Time scales of lipid dynamics and molecular dynamics. *In* Biological Membranes: A Molecular Perspective from Computation and Experiment. K. M. Merz and B. Roux, editors. Birkhäuser, Boston. 3–29.

Pearlman, D. A., D. A. Case, J. W. Caldwell, W. S. Ross, T. E. Cheatham, D. M. Ferguson, G. L. Seibel, U. C. Singh, P. K. Weiner, and P. A. Kollman. 1995. AMBER, Version 4.1. Department of Pharmaceutical Chemistry, University of California, San Francisco.

Pfeiffer, W., T. Henkel, E. Sackmann, W. Knoll, and D. Richter. 1989. Local dynamics of lipid bilayers studied by incoherent quasi-elastic neutron scattering. *Europhys. Lett.* 8:201–206.

Pickar, A. D., and R. Benz. 1978. Transport of oppositely charged lipophilic probe ions in lipid bilayer membranes having various structures. *J. Membr. Biol.* 44:353–376.

Rand, R. P., and V. A. Parsegian. 1989. Hydration forces between phospholipid bilayers. *Biochim. Biophys. Acta.* 988:351–376.

Ruocco, M. J., and G. G. Shipley. 1982. Characterization of the subtransition of hydrated dipalmitoylphosphatidylcholine bilayers. *Biochim. Biophys. Acta.* 691:309–320.

Ryckaert, J.-P., and A. Bellemans. 1975. Molecular dynamics of liquid *n*-butane near its boiling point. *Chem. Phys. Lett.* 30:123–125.

Ryckaert, J.-P., G. Ciccotti, and H. J. C. Berendsen. 1977. Numerical integration of the Cartesian equation of motion of a system with constraints: molecular dynamics of *n*-alkanes. *J. Comp. Phys.* 23: 327–341.

Sackmann, E. 1995. Physical basis of self-organization and function of membranes: physics of vesicles. *In* Handbook of Biological Physics, Vol. 1A, Structure and Dynamics of Membranes. R. Lipowsky and E. Sackmann, editors. Elsevier, Amsterdam. 213–304.

Saffman, P. G., and M. Delbrück. 1975. Brownian motion in biological membranes. *Proc. Natl. Acad. Sci. USA.* 72:3111–3113.

Shinoda, W., N. Namiki, and S. Okazaki. 1997. Molecular dynamics study of a lipid bilayer: convergence, structure and long-time dynamics. *J. Chem. Phys.* 106:5731–5743.

Singer, S. J., and G. L. Nicolson. 1972. The fluid mosaic model of the structure of cell membranes. *Science.* 175:720–731.

Szabo, A. 1984. Theory of fluorescence depolarization in macromolecules and membranes. *J. Chem. Phys.* 81:150–167.

Tieleman, D. P., S. J. Marrink, and H. J. C. Berendsen. 1997. A computer perspective of membranes: molecular dynamics studies of lipid bilayer systems. *Biochim. Biophys. Acta.* 1331:235–270.

Tobias, D. J., K. Tu, and M. L. Klein. 1997. Atomic-scale molecular dynamics simulations of lipid membranes. *Curr. Opin. Colloid Interface Sci.* 2:15–26.

Zannoni, C. 1994. An introduction to the molecular dynamics method and to orientational dynamics in liquid crystals. *In* The Molecular Dynamics of Liquid Crystals. G. R. Luckhurst and C. A. Veracini, editors. Kluwer, Dordrecht. 139–169.